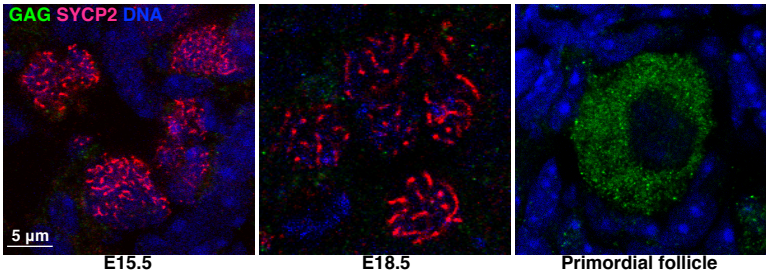

Figure S1. Expression of IAP GAG protein, related to Figure 1.

IAP-encoded GAG expression is barely detected in fetal oocytes but is apparent in primordial follicle. Sections of E15.5, E18.5 and adult WT ovaries were probed with IAP GAG (green) and SYCP2 (red) antibodies.

A

L1 FL families	Normalized mapped reads				KO1,2/WT1,2
	WT1	WT2	KO1	KO2	
A	12,095,268	14,857,217	26,013,205	26,125,852	1.934
F	40,065	48,007	75,331	96,386	1.950
G.F	2,481,752	3,298,293	6,462,968	6,141,762	2.181
T.F	14,107,623	16,154,873	27,883,787	28,697,969	1.820
n/a	666,585	736,671	1,259,739	1,294,649	1.870

B

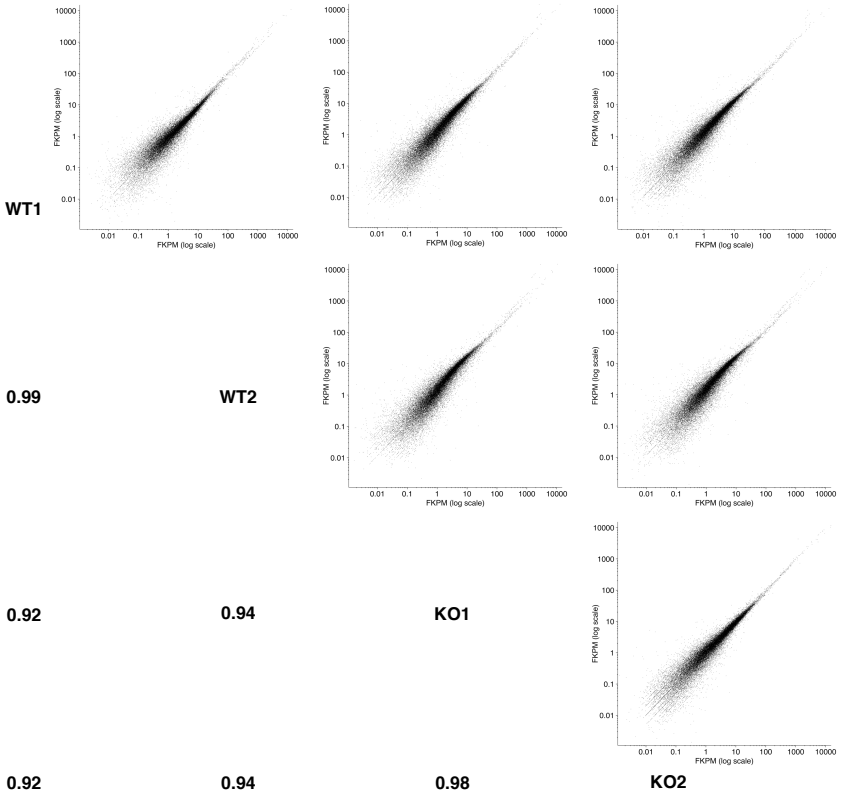

Figure S2. RNA-Seq analysis of gene expression in Mael-null E15.5 ovaries, related to Figure 2 and Table S1.

(A) Normalized counts of mapped sequenced reads to different L1 families (A, F, G.F and T.F) in WT and *Mael*-mutant E15.5 ovaries. n/a - reads that could not be mapped uniquely to a single L1 family.

(B) Correlation charts and Pearson's *r* correlation coefficients of gene expression in WT and *Mael*-mutant E15.5 ovaries (two biological replicates) determined by RNA-Seq.

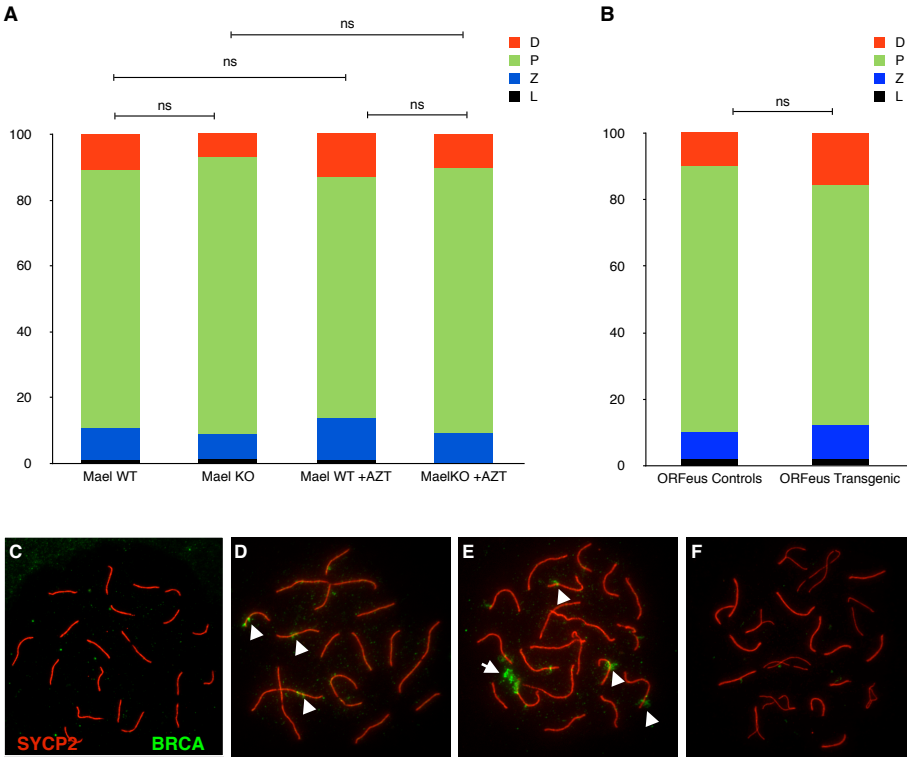

Figure S3. MPI progression, MSUC and asynapsis in fetal oocytes under different experimental conditions of analysis, related to Figures 4, 6 and 7 and Tables S3.

(A), (B) Nuclear spreads of meiotic prophase I E18.5 oocytes of indicated genotypes were immunostained for SYCP1 and SYCP2 proteins and classified based on the extent of assembly and appearance of axial/lateral elements of the meiotic chromosome core and synaptonemal complex. (Chi square test, ns - P>0.05).

(C) WT E18.5 oocytes with complete synapsis (visualized with SYCP2 antibody) and no MSUC (visualized with BRCA1 antibody).

(D) WT E18.5 oocyte with apparently complete synapsis but with small areas of MSUC (arrowheads).

(E) WT E18.5 oocyte with limited asynapsis and associated MSUC (arrow), and MSUC in areas with apparently normal synapsis (arrowheads).

(F) WT E18.5 oocyte with extensive asynapsis and no evidence of MSUC.

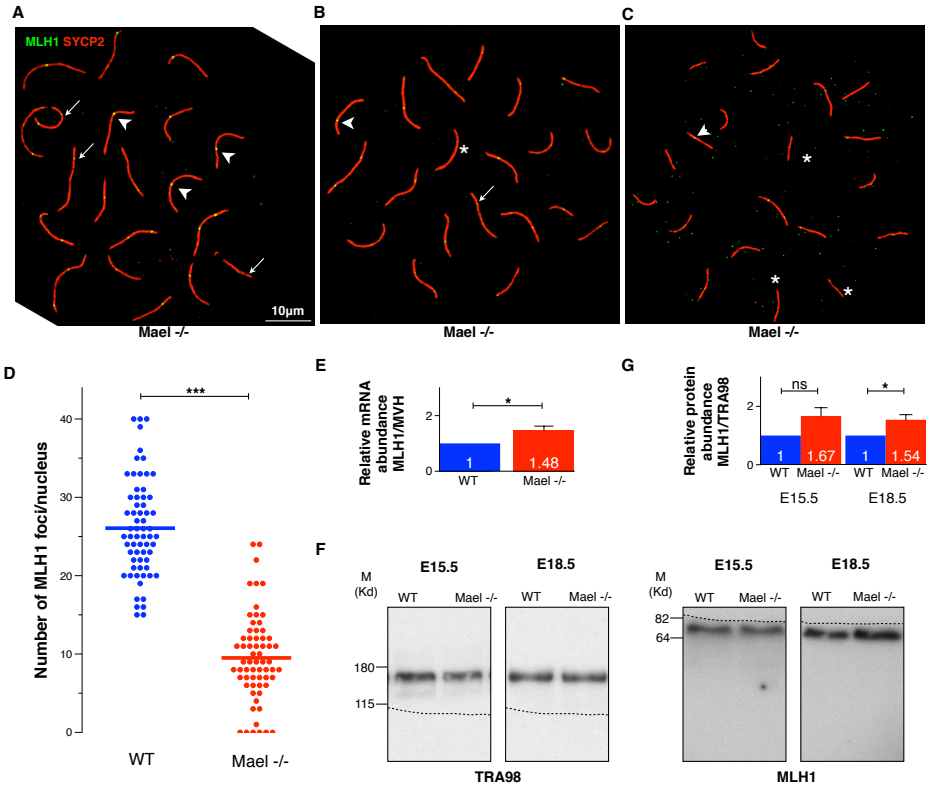

Figure S4. Localization and quantification of MLH1 expression in E18.5 fetal oocytes, related to Figure 5 and Table S4.

(A-C) Additional images of normal and defective appearance of prospective crossovers (assessed with MLH1 antibody) on synaptonemal complexes (marked by SYCP2 labeling in red) in *Mael*-null E18.5 pachytene nuclei. Arrowheads show MLH1 foci (green) of normal intensity. Defective patterns included synaptonemal complexes decorated with MLH1 foci of diminished intensity (arrows) or lacking MLH1 foci entirely (asterisks).

(D) Distribution of the number of MLH1 foci on synaptonemal complexes in WT and *Mael*-null E18.5 pachytene nuclei. Bar indicates mean. (Two-tailed unpaired Student's t-test, ***-P<0.001).

(E) Abundance of MLH1 mRNA relative to Mouse Vasa Homolog (MVH) mRNA levels as determined by real-time RT-PCR.

(F, G) Western blot analysis (F) and quantification (G) of protein lysates of WT and *Mael*$^{-/-}$ E15.5 and E18.5 ovaries using antibodies MLH1 and TRA98 (germ cell-specific marker). Dashed line marks cut lines of membranes before probing with different antibodies. Mean ± St.dev. from three independent measurements are shown (two-tailed unpaired Student's t-test, ns-$P>0.05$; *-$P<0.05$).

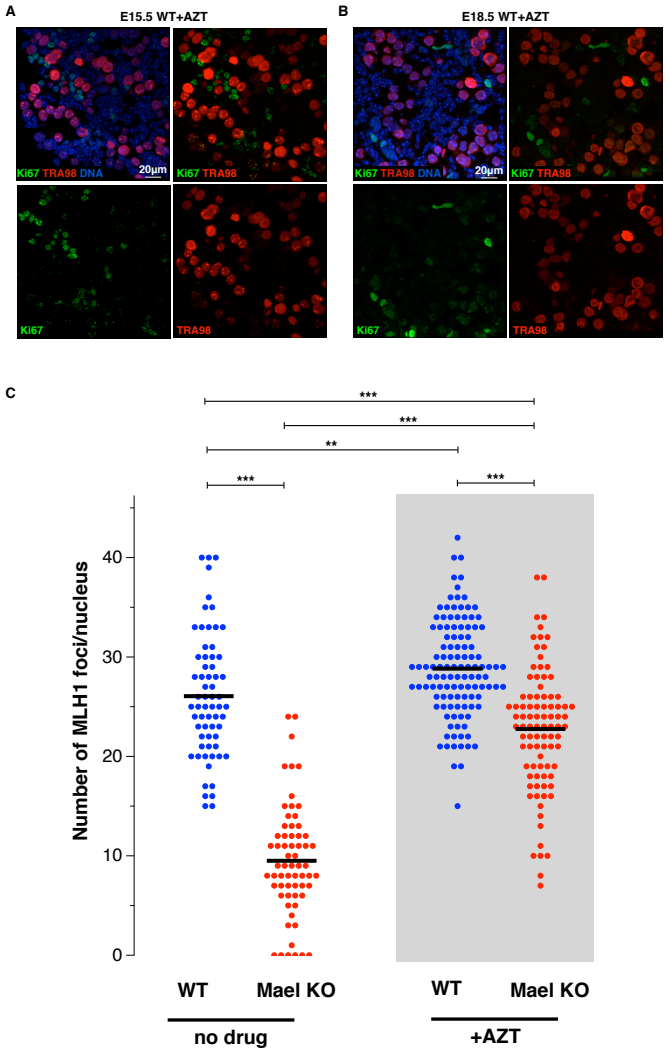

Figure S5. Effects of AZT on proliferation and MLH1 foci fetal oocytes, related to Figure 7 and Tables S4 and S7.

(A, B) Immunostaining of sections of AZT-treated E15.5 (A) and E18.5 (B) WT ovaries with Ki67 (cell proliferation marker, green) and TRA98 (oocyte specific marker, red). Individual panels show images of single or merged channels. DNA (detected with DAPI) – blue.

(C) Distribution of the number of MLH1 foci on synaptonemal complexes in WT and *Mael*-null E18.5 pachytene nuclei. Bars indicate mean. (Two-tailed unpaired Student's t-test, **-$P<0.01$; ***-$P<0.001$).

Supplemental Table Legends

Table S1. Results of RNA-Seq and GeneOntology analyses in WT and *Mael*-null E15.5 ovaries, related to Figure S2.

Table S2. Quantification and statistical analysis of oocyte counts and L1ORF1p nuclear levels in WT and *Mael*-null ovaries, related to Figure 3.

Table S3. Quantification and statistical analysis of meiotic prophase I distribution of WT and *Mael*-null E18.5 oocytes under different experimental conditions, related to Figure S3.

Table S4. Quantification and statistical analysis of meiotic events, crossover and follicular counts in WT and *Mael*-null ovaries, related to Figures 4, 5, S4 and S5.

Table S5. Quantification and statistical analysis of aneuploidy and viability of WT embryos and *Mael* +/- preimplantation embryos obtained from *Mael*-null oocytes fertilized with WT sperm, related to Figure 5.

Table S6. Quantification and statistical analysis of oocyte counts, L1ORF1p nuclear levels, meiotic events and crossovers in control and tet-ORFeus doxycycline-treated ovaries, related to Figure 6.

Table S7. Quantification and statistical analysis of oocyte counts, L1ORF1p nuclear levels, meiotic events and crossovers in control and AZT-treated WT and *Mael*-null ovaries, related to Figure 7 and S5.

Supplemental Experimental Procedures

Fertility analysis

We mated wild-type C57BL/6J males with 2-6 months old *Mael*-null females or control wild-type siblings. We caged one female with one male and examined her daily for the presence of vaginal plugs in the morning. We recorded the day of the plug appearance as day 0.5 post coitum, referred to as "0.5 dpc". We monitored cages daily and recorded the number and size of litters.

Superovulation and isolation of oocytes, and pre-implantation embryos

We superovulated wild-type and *Mael*$^{-/-}$ females (2-6 months old) by intra-peritoneal injection of 0.5 IU of PMSG (Calbiochem-EMD Chemical) followed by injection of 5 IU of hCG (Calbiochem-EMD Chemical) 48 hrs later and mated, when necessary, with wild type males. We collected GV oocytes from disaggregated ovaries 48h after PMSG and ovulated oocytes from oviducts 24h after the hCG injection. To assess preimplantation development, we sacrificed pregnant female mice at 1.5 or 3.5 dpc and flushed out embryos from the oviduct and uterus, respectively, with M2 media (Chemicon).

Tissue collection and histological analysis

We fixed freshly dissected ovaries in 4% PFA/PBS1X fixative (EMS) overnight at room temperature. We embedded ovaries in paraffin, sectioned at an 8 μm thickness and stained slides with hematoxylin and eosin (SIGMA).

Cryosections

We fixed dissected embryonic and adult ovaries in freshly prepared 2% PFA (EMS) in PBS at 4°C for 2 hrs. We washed samples through a sucrose gradient (10%, 20%, 30% in PBS),

embedded in Tissue-Tek OCT (Finetek, Sakura) and stored at -80°C. We cryosectioned 8µm-samples for further analysis.

Preparation of chromosome spreads

We prepared chromosome spreads of mouse oocytes during prophase I using previously described methods with some modifications (Hodges & Hunt, 2002; Peters et al, 1997). Briefly, we dissected and placed embryonic ovaries in a hypotonic buffer (30 mM Tris-Cl (pH 8.2), 50 mM sucrose, 17 mM sodium citrate) for 45 min on ice. We then transferred ovaries to 50 µl of 100 µM sucrose (pH 8.2) and gently rasped them with two forceps to obtain a cell suspension. We placed the cell suspension on a glass slide previously immersed in fixative (1% PFA, 0.15% Triton X-100, pH 9.2 adjusted with borate). We dispersed the cells on the slide by tilting and then slowly dried the slide for 2 hrs in a humidified box. We washed the slides in water containing 0.08% Photo-Flo (Kodak).

We prepared metaphase I and metaphase II chromosome spreads from *in vitro* cultured GV and ovulated oocytes, respectively, as follows. We removed zona pellucida by incubating oocytes in acidic Tyrod's solution (Chemicon) for ~2 min, followed by 3 washes in M2 medium. We placed zona pellucida-free oocytes lacking polar bodies in a hypotonic solution (10% Na citrate, 25% fetal calf serum diluted by water) at 37°C for 5-10 min, then transferred into a drop of fixative (1% PFA, 0.15% Triton -100, 3 mM dithiothreitol, pH 9.2 adjusted by borate) on a slide glass and then slowly dried the sample. We washed the slides in water containing 0.08% Photo-Flo (Kodak).

Immunofluorescence

We washed cryosections or nuclear spread slides for 15 min in (PBS, 0.05% Triton X-100) and incubated for 1 hr at RT with blocking solution (PBS, 0.05% Triton X-100, 10% Normal

serum, 3% BSA). We applied antibodies at appropriate dilutions in the blocking solution and incubated overnight at 4°C. We washed slides the next day in (PBS, 0.05% Triton X-100) for 5 min, followed by two 10 min washes in PBS. We detected primary antibodies by incubating slides for 2 hrs at room temperature with corresponding secondary antibodies. After incubation, we washed the slides in (PBS, 0.05% Triton X-100) for 5 min, followed by two 10 min washes in PBS, and counterstained with DAPI. We used Vectashield (Vector) as antifading mounting solution.

For whole mount immunostaining, we fixed dissected embryonic ovaries in freshly prepared 2% PFA (EMS) in PBS at 4°C for 2 hrs. We washed ovaries for 3x30 min in (PBS, 0.1% Triton X-100) and incubated on a nutator overnight at 4°C with blocking solution (PBS, Triton 0,1%, Glycine 0,15%, 10% Normal serum, BSA 3%). We applied antibodies at appropriate dilutions in the blocking solution and incubated overnight at 4°C on a nutator. We washed ovaries the next day for 3x30 min in (PBS, 0.1% Triton X-100). We detected primary antibodies by incubating ovaries overnight at 4°C with corresponding secondary antibodies. After incubation, we washed samples for 3x30 min in (PBS, 0.1% Triton X-100), and counterstained with DAPI. We mounted ovaries between slides and coverslips and we used Vectashield (Vector) as anti-fading mounting solution.

Microscopy

We used a Nikon Eclipse E800 microscope equipped with a Diagnostic Instruments model 2.3.1 digital camera for imaging histological sections. We collected images of nuclear spreads on a Olympus BX61 microscope equipped with a Hamamatsu C4742-95 digital camera. For imaging of ovarian sections (single photon) and wholemount immunostained ovaries (two-photon), we used TCS-SP5 laser-scanning confocal microscope (Leica, Buffalo

Grove, IL). We performed image analysis using ImageJ (http://rsbweb.nih.gov/ij/), Photoshop (Adobe Systems, Inc.), SlideBook (Intelligent Imaging Innovations, Inc.), LAS AF (Leica Microsystems CMS GmbH), MetaMorph (Molecular Devices, Inc.) and Imaris (Bitplane).

Immunoblotting

We prepared protein lysates from 3 to 5 pairs of embryonic gonads of appropriate genotypes in lysis buffer [50mM Tris pH 7.5, 150mM NaCl, 0.1%NP40, 1mM DTT, 20mM PMSF, Halt protease and phosphatase cocktail inhibitors 100X (Thermo Scientific)]. We determined protein concentration using BCA (Thermo Scientific). We used MetaMorph (Molecular Devices, Inc.) software to quantify relative density of individual protein bands.

Antibodies

We used the following antibodies at indicated dilutions: rabbit polyclonal anti-MAEL (1:1000 for immunofluorescence and 1:10000 for Western blot) (Soper et al, 2008); rabbit polyclonal anti-L1ORF1p 1:500 for immunofluorescence and 1:2000 for Western blot) (Martin & Branciforte, 1993; Soper et al, 2008); rat polyclonal anti-TRA98 (1:500 for immunofluorescence and 1:2000 for Western blot) (B-Bridge International, INC, Cat#: 73-003); rabbit polyclonal anti-IAPgag (1:500 for IF, gift of B.R. Cullen) (Aravin et al, 2009), mouse monoclonal anti-γH2AX (1:1000, Upstate; #05-636); rabbit polyclonal anti-SYCP1(1:1000, Abcam); guinea pig polyclonal anti-SYCP2 (1:1000, gift of P.J. Wang) (Yang et al, 2006); rabbit polyclonal anti-SYCP3 (1:750, Abcam; ab15092); anti-hRAD51 (1:300, gift of R. Kanaar); mouse monoclonal anti-α-Tubulin (1:1000, Sigma-Aldrich, Cat#: T9026), rabbit polyclonal anti-BRCA1 (1:1500, gift of S. Namekawa) (Ichijima et al, 2011), rabbit polyclonal anti-Ki67 (1:500, Abcam, cat#: ab15580). We used the following secondary

antibodies: Alexa donkey ant- rabbit 488 (Invitrogen, cat#:A-21206**),** Alexa donkey ant-rabbit 568 (Invitrogen, cat#:A10042), Alexa donkey ant- guinea pig 568 (Invitrogen, cat#:A11075), Alexa donkey ant- mouse 488 (Invitrogen, cat#:A21202), Alexa Donkey anti-Rat 488 (Jackson Immunoresearch, cat#:712-545-153), Alexa Goat Anti-rat 568 (Invitrogen, cat#:A-11077**);** Alexa donkey-anti-rabbit, Alexa donkey-anti-guinea pig, and donkey-anti-mouse, 488 and 594 (Molecular Probes). All secondary antibodies were used at a 1:500 dilution.

Real-time RT-PCR

We isolated total ovarian RNA using TRIZOL reagent (Invitrogen) and treated it with TURBO DNA-free (Ambion) as per manufacturer's recommendations. We used RNA for cDNA synthesis with random hexamer primers and SuperScript III Reverse Transcriptase (Invitrogen). We diluted the resulting cDNA in water for downstream PCR reactions using iQ SYBR Green Supermix (Bio-Rad) performed in triplicate. We performed real-time PCR using MJResearch DNA Engine Opticon to detect SYBR Green. We generated a standard curve using a serial dilution and actin was used for normalization. Primers for real-time PCR used were F-act: TGG GAA TGG GTC AGA AGG ACT, R-act: GGG TCA TCT TTT CAC GGT TGG C; F-mlh1: AAC TGC AGA CTT TTG AGG ATT TA, R-mlh1: CAT TTC CCA TCA GCT GTT TT; F-mvh: TGG CAG AGC GAT TTC TTT TT, R-mvh CGC TGT ATT CAA CGT GTG CT; F-line1 5` UTR: GGC GAA AGG CAA ACG TAA GA, R-line1 5` UTR: GGA GTG CTG CGT TCT GAT GA; F-IAPGag: AAC CAA TGC TAA TTT CAC CTT GGT, R-IAPGag: GCC AAT CAG CAG GCG TTA GT. We analyzed relative quantitation using ΔΔCt methods.

Supplemental References

Aravin AA, van der Heijden GW, Castaneda J, Vagin VV, Hannon GJ, Bortvin A (2009) Cytoplasmic compartmentalization of the fetal piRNA pathway in mice. *PLoS Genet* **5:** e1000764

Hodges CA, Hunt PA (2002) Simultaneous analysis of chromosomes and chromosome-associated proteins in mammalian oocytes and embryos. *Chromosoma* **111:** 165-169

Ichijima Y, Ichijima M, Lou Z, Nussenzweig A, Camerini-Otero RD, Chen J, Andreassen PR, Namekawa SH (2011) MDC1 directs chromosome-wide silencing of the sex chromosomes in male germ cells. *Genes & development* **25:** 959-971

Langmead B, Trapnell C, Pop M, Salzberg SL (2009) Ultrafast and memory-efficient alignment of short DNA sequences to the human genome. *Genome biology* **10:** R25

Martin SL, Branciforte D (1993) Synchronous expression of LINE-1 RNA and protein in mouse embryonal carcinoma cells. *Molecular and cellular biology* **13:** 5383-5392

Penzkofer T, Dandekar T, Zemojtel T (2005) L1Base: from functional annotation to prediction of active LINE-1 elements. *Nucleic acids research* **33:** D498-500

Peters AH, Plug AW, van Vugt MJ, de Boer P (1997) A drying-down technique for the spreading of mammalian meiocytes from the male and female germline. *Chromosome Res* **5:** 66-68

Soper SF, van der Heijden GW, Hardiman TC, Goodheart M, Martin SL, de Boer P, Bortvin A (2008) Mouse maelstrom, a component of nuage, is essential for spermatogenesis and transposon repression in meiosis. *Dev Cell* **15:** 285-297

Tilly JL (2003) Ovarian follicle counts--not as simple as 1, 2, 3. *Reprod Biol Endocrinol* **1:** 11

Trapnell C, Pachter L, Salzberg SL (2009) TopHat: discovering splice junctions with RNA-Seq. *Bioinformatics* **25:** 1105-1111

Trapnell C, Williams BA, Pertea G, Mortazavi A, Kwan G, van Baren MJ, Salzberg SL, Wold BJ, Pachter L (2010) Transcript assembly and quantification by RNA-Seq reveals unannotated transcripts and isoform switching during cell differentiation. *Nature biotechnology* **28:** 511-515

Yang F, De La Fuente R, Leu NA, Baumann C, McLaughlin KJ, Wang PJ (2006) Mouse SYCP2 is required for synaptonemal complex assembly and chromosomal synapsis during male meiosis. *J Cell Biol* **173:** 497-507

Zemojtel T, Penzkofer T, Schultz J, Dandekar T, Badge R, Vingron M (2007) Exonization of active mouse L1s: a driver of transcriptome evolution? *BMC Genomics* **8:** 392

Zheng Q, Wang XJ (2008) GOEAST: a web-based software toolkit for Gene Ontology enrichment analysis. *Nucleic acids research* **36:** W358-363